TITLE

Four neurons pattern brain-wide developmental activity through neuropeptide signaling.

Authors

Jun Reichl[1], Julia M. Miller[1], Harpreet Randhawa[2], Lesly M. Palacios Castillo[3], and Orkun Akin[2]*

Affiliations

[1] Neuroscience Interdepartmental Graduate Program, University of California, Los Angeles, Los Angeles, CA, USA

[2] Department of Neurobiology, David Geffen School of Medicine at UCLA, University of California, Los Angeles, Los Angeles, CA, USA

[3] Molecular, Cellular, and Integrative Physiology Interdepartmental Graduate Program, University of California, Los Angeles, Los Angeles, CA, USA

* Correspondence: akin.orkun@gmail.com

ABSTRACT

In both vertebrates and invertebrates, the developing brain becomes electrically active before it is ready to process sensory input[1–4]. During neural circuit maturation, developmental activity is thought to refine synaptic connections by driving neuronal co-activation in rhythmic patterns[5]. Here we describe cellular interactions that shape brainwide developmental activity and their molecular basis. In *Drosophila*, patterned stimulus independent neural activity (PSINA) engages the entire brain in highly stereotyped, globally coordinated cycles of activity[6]. A molecularly-defined population of ~2,000 neurons (Transient Receptor Potential Gamma, *Trpγ*+ neurons) act as an activity template for PSINA. We show that this activity template is patterned by four neurons expressing the neuropeptide SIFamide (SIFa)[7]. Signaling through the SIFa Receptor[8], SIFa modulates the activity of both SIFa and *Trpγ*+ neurons to establish the brainwide activity cycles of PSINA. In turn, *Trpγ*+ neurons sustain SIFa neuron activity through a recurrent interaction. Neuropeptides modulate neuronal activity through synapse-free, or wireless, signaling[9]; a fitting mode of communication for a process tasked with refining on-going synapse formation. By placing neuropeptide signaling at the core of developmental activity, this work highlights the rich neurophysiological potential of the chemical connectome in shaping the developing brain.

INTRODUCTION

Around the onset of synaptogenesis, before the nervous system is ready to process sensory input, the developing brain turns on with waves of patterned rhythmic activity. Such developmental activity has been seen in many parts of the mammalian brain, including the visual, auditory, and olfactory systems, the spinal cord, thalamus, and the cortex[1–3]. Altering the activity in sensory systems, where it has been studied in greatest depth, leads to disruptions in topographic mapping[10–12] and circuit function[13,14]. Changes to the activity in the developing cortex are thought to be linked to neurodevelopmental disorders[2], highlighting the significance of understanding how this process contributes to the assembly of the brain. While specifics are outstanding, and likely to be case-specific, the consensus view is that the activity acts by mediating neuronal co-activation[5]: Selective strengthening or weakening of synapses through Hebbian plasticity[15]. This framework elevates the importance of the spatiotemporal patterns of activity[16] and, by extension, the mechanisms which generate them.

The discovery of similar activity in the developing brain of the fruit fly *Drosophila melanogaster*[6,17] indicates that this phenomenon is fundamental to neurodevelopment. The adult fly brain is built during the 100 hours of metamorphosis, or pupal development. Patterned, stimulus-independent neural activity (PSINA, *'see-nah'*) starts ~50 hours after puparium formation (hAPF)[6], co-incident with the appearance of the first structural synapses[18,19]. For the following two days until an hour before the adult fly emerges, PSINA engages the whole brain in cycles of activity comprising globally coordinated active and silent phases (Fig.1a-c). Embedded within each global active phase are stereotyped cell-type-specific activity patterns which are more correlated between future synaptic partners[6].

PSINA relies on a population of ~2,000 neurons, genetically defined by their expression of the cation channel Trpγ[20]. Loss of *trpy* gene function alters PSINA patterns both across the brain and at the single cell-type-level and disrupts synaptic development in a non-cell autonomous manner. Brainwide PSINA in *trpγ* mutants mirrors the activity recorded from *Trpγ*+ neurons[20], indicating that this small population acts as an activity template for the rest of the brain.

Here, we report that the *Trpγ+* activity template is modulated by the neuropeptide SIFa. SIFa is a highly conserved[21] arthropod neuropeptide produced principally by four neurons in the Pars Intercerebralis (PI) region[7,22](Fig.1d), a neuroendocrine command center homologous to the mammalian hypothalamus. SIFa neurons (aka DNc01/2[23]) are present in the larva and undergo extensive remodeling during pupal development to extend processes throughout the adult brain and ventral nerve cord[7]. The SIFa Receptor, SIFaR[8], is a G protein-coupled receptor expressed broadly throughout the brain (Fig.1d). In the adult, SIFa-SIFaR signaling has been implicated in a range of adult behaviors, including feeding[24], activity rhythms[25], sleep[26,27], and courtship[7,28]. We find that, during pupal development, this signaling module acts on *Trpγ+* neurons to pattern the brainwide activity cycles of PSINA. By identifying four defined neurons that shape brainwide activity through a specific ligand-receptor interaction, our work brings into focus a genetically-programmed neural engine of discrete composition driving this fundamental phase of neurodevelopment.

RESULTS

To observe PSINA, we use a live imaging approach we term the widefield assay. We use genetically encoded calcium indicators to visualize neural activity: GCaMP6s[30] for single cell class recording (e.g., pan-neuronal for brainwide PSINA), and GCaMP6s and RCaMP1b[31] when imaging two different classes of cells. For independent genetic access to different classes of cells, we use the GAL4-UAS[32] and LexA-LexAop[33] expression systems. When needed, we control the timing of GAL4-driven expression using GAL80ts[34], which inhibits GAL4 at 18°C, but allows for full expression at 29°C. Below, we refer to this approach as temporally-targeted expression. We stage and genotype flies at the onset of pupal development, and, at ~50hAPF, prepare them for imaging by removing the cuticle around their heads (Fig.1a,b). Using a standard long-working-distance fluorescence microscope, we can record simultaneously from up to 80 pupae for two days; that is, until the flies complete metamorphosis and emerge as adults. This medium-throughput assay made it possible to carry out the neuropeptide screen which identified *SIFa*.

SIFa and SIFaR are necessary for PSINA cycles

In *SIFa* mutants, PSINA has lower signal intensity and altered duty cycle, with less time active per hour during early stages (65-75hAPF) shifting to more time active after ~75hAPF (Fig.1e,f). Most prominently, the temporal organization of the activity is altered: In the wildtype, PSINA is organized into cycles of active and silent phases with periods of 10-15 minutes (Fig.1c). We visualized these cycles in the frequency domain by taking the Fourier transform of the PSINA traces and calculating the power spectral density (PSD); the PSD displays how the power in the original signal is distributed across different frequencies. (The power of a time-domain signal is proportional to the square of its amplitude.) Most of the power in wildtype PSINA is carried by a band around 10^{-3}Hz (Fig.1g, 1st column), which corresponds to the 10-15 minute cycle period. Using the PSD representation, we compared wildtype and experimental (Fig.1g, 2nd column) sets of traces across pupal development and found that the 10^{-3}Hz band is largely absent in *SIFa* mutants (Fig.1g, *SIFa[1],* 3rd column, bottom panel). These frequencies where wildtype and *SIFa* mutant PSINA are different account for ~50% of the signal power in the wildtype (Fig.1g, *SIFa[1],* 3rd column, top panel). In effect, the cycles are lost in *SIFa* mutants. Complementation analysis with a deficiency and rescue with a chromosomal duplication confirmed that the used alleles are true nulls and the phenotype is monogenic in origin, respectively (Fig.1e-g, Fig.S1a). We conclude that *SIFa* is necessary for the stereotyped activity cycles of PSINA.

SIFaR is the only known receptor for SIFa[8]. Paired with a deficiency, a $SIFaR^{null}$ allele leads to the same PSINA phenotypes we observed in SIFa mutants (Fig.1h-j): altered duty cycle, reduced signal, and lost cycles. We tested a protein trap, $SIFaR^{GFSTF}$, and a gene trap GAL4 driver, $SIFaR^{G4}$, in combination with $SIFaR^{null}$ and saw similar changes to PSINA, indicating that these are strong loss-of-function (LoF) alleles (Fig.1h-j, Fig.S1b-d). Hereafter, we refer to $SIFaR^{GFSTF}$ as $SIFaR^{LoF}$. As with *SIFa*, rescue with a chromosomal duplication confirmed the monogenic origin of the *SIFaR* phenotypes (Fig.1h-j, Fig.S1b-d). We conclude that *SIFaR* is necessary for wildtype PSINA.

To ask how *SIFa* and *SIFaR* interact, we carried out double mutant analysis using *SIFa[1]* homozygotes and heteroallelic combinations of $SIFaR^{null}$ with $SIFaR^{LoF}$ or $SIFaR^{G4}$ (Fig.S1e-g,h-j). The *SIFaR* single mutants, particularly those carrying the $SIFaR^{G4}$ allele did differ from the double mutants in how they affected duty cycle and average signal. We attribute the differences to these *SIFaR* alleles not being complete nulls. However, for the most prominent phenotype—loss of cycles—the single mutants were indistinguishable from the doubles. The absence of an additive effect is consistent with SIFa and SIFaR functioning as an exclusive ligand-receptor module in PSINA.

SIFa gene function and SIFa neuronal activity are necessary during PSINA

To ask whether *SIFa* is necessary during PSINA, we used a GAL4 driver which specifically labels the four large SIFa neurons in the PI[22] (*SIFa*^{G4} [7], Fig.S2a) to knockdown *SIFa* expression (Fig.2a) in a temporally targeted manner. The resulting PSINA phenotypes were comparable to that seen in the mutants (Fig.2b,c, Fig.S2b) indicating that the SIFa neuropeptide is required during PSINA.

Neuropeptidergic signaling operates alongside co-transmission of other neuroactive compounds[29]. We asked if electrical silencing, by exacerbating the *SIFa* mutant PSINA phenotype, would reveal a co-transmitter requirement in SIFa neurons. Contrary to expectation, *SIFa*^{G4} driven KiR2.1 expression resulted in a weaker PSINA phenotype (Fig.2d,e, Fig.S2c). We tested two other GAL4s which label the SIFa neurons, *SIFa*$^{G4\text{-}2}$ [30] and *SIFa*$^{G4\text{-}3}$ (Fig.2d,e, Fig.S2c,e-h). Temporally-targeted KiR2.1 expression by all three drivers altered PSINA in similar fashion, and *SIFa*$^{G4\text{-}2}$ led to a more penetrant phenotype, matching and not exceeding the severity of the *SIFa* mutation. We conclude that *SIFa* expression is the dominant contribution of SIFa neurons to PSINA.

SIFaR gene function during pupal development is necessary and sufficient for PSINA

To test when *SIFaR* gene function is necessary, we targeted RNAi knockdown to pupal development (Fig.2f,g, Fig.S2d). Knockdown with the pan-neuronal *PanN*^{G4} driver phenocopied the *SIFaR* mutant phenotype. The effect with *SIFaR*^{G4} was weaker, likely due to the dependence of gene trap expression to transcription from the native locus. Notably, knockdown of *SIFaR* with the *SIFa*^{G4} driver and the *Trpγ*^{G4} gene trap also disrupted PSINA, indicating that the receptor is necessary in these neuronal populations. In keeping with this, we found that *SIFaR*^{G4} labels SIFa neurons starting at mid-pupal development (Fig.S3). We conclude that SIFaR gene function is necessary during PSINA.

We assessed the fidelity of the *SIFaR*^{G4} gene trap in capturing the functional expression domain of *SIFaR* in a rescue experiment. Temporally-targeted expression of *UAS-SIFaR*[27] with *SIFaR*^{G4} or *PanN*^{G4} at >28°C led to an overexpression phenotype (Fig.S4a-d): Beyond restoring the lost cycles, both drivers increased the duty cycle and average signal due to extended active phases. We were able more closely match wildtype PSINA by rearing the animals at a lower temperature (Fig.S4e-g). Under both conditions, *SIFaR*^{G4} and *PanN*^{G4} yielded comparable results, indicating that the gene trap captures the functional expression domain of *SIFaR*. We conclude that *SIFaR* expression during pupal development is sufficient for wildtype PSINA.

SIFaR in the central brain is necessary for cycles

We asked where in the developing brain SIFaR receptor function is necessary for wildtype PSINA. *SIFaR*^{G4} captures an expression domain that expands through pupal development to encompass many thousands of neurons (Fig.S3). This is consistent with a recent fluorescence *in situ* hybridization based characterization of *SIFaR* transcript localization[22]. Silencing the *SIFaR*^{G4} domain with KiR2.1 leads to complete loss of PSINA (Fig.2h). The fly optic lobes (OLs) are positioned as satellite neuropils whose spatial separation from the central brain (CB) make it possible to assess distinct participation in PSINA (Fig.1a,d). We had previously targeted KiR2.1 silencing to either the CB or OLs using conditional *GAL80* constructs and a mostly OL-specific FLP recombinase to find that only the CB subset of *Trpγ+* neurons is necessary for wildtype PSINA[20]. Using a similar genetic scheme (Fig.3a), we carried out spatially targeted KiR2.1 silencing experiments with *PanN*^{G4}, *Trpγ*^{G4}, or *SIFaR*^{G4} (Fig.3b-e). Silencing the CB complement of these expression domains virtually abolished PSINA in both the CB and the OLs (Fig.3c,d). Silencing the OL complements reduced signal in the OLs by 50-75% and in the CB by ~30% without altering PSINA cycles in either spatial domain (Fig.3c,e). The non-local effect of OL silencing on signal in the CB may be due to the incompleteness of our spatial fractionation approach or to feedforward connections between the OL and the CB. These results indicate that the CB complement of all three drivers, including *SIFaR*^{G4}, contain neuronal populations whose activity is necessary for PSINA across the brain.

We used the same approach to knock down *SIFaR* expression in either the CB or the OLs (Fig.3f-h). Consistent with the silencing results, knockdown in either spatial domain reduced PSINA signal. However, only CB knockdown led to the alteration of cycles across the brain (Fig.3f,g). We conclude that while *SIFaR* is used throughout the brain to support wildtype signal amplitude, it is necessary only in the CB for PSINA cycles.

SIFa neurons pattern brainwide PSINA

We next sought to determine the relationship between the activity of SIFa neurons and brainwide PSINA. The proximity of the oversized SIFa neuronal soma to the dorsal surface of the head made it possible to record from these cells in the widefield assay (Fig.4a). GCaMP6s signal from SIFa neurons revealed an activity profile broadly comparable to brainwide PSINA, which we followed in parallel using RCaMP1b: At the level of cycles, SIFa neuron activity is very similar to brainwide PSINA in wildtype animals (Fig.4b,d). Closer inspection revealed

that SIFa neuron activity cycles both initiate before and end after brainwide cycles throughout the duration of PSINA (Fig.4b,e). Measuring the SIFa neuron lead, we found that it starts out at tens of seconds, levels to several seconds by 80hAPF, and remains detectable until eclosion (Fig.4e).

SIFa neuron activity and brainwide PSINA remain coupled in *SIFa* mutants. Across different parts of the brain (CB v OL), PSINA is highly correlated in both wildtype and *SIFa* mutant animals (Fig.4f), suggesting that the brainwide activity template[20] persists in the absence of *SIFa*. In the wildtype, SIFa neuron activity and brainwide PSINA recorded from the same region-of-interest is also well-correlated (Fig.4g). However, the lack of sweep-to-sweep correspondence between these activity profiles reduces the correlation relative to what we observe across the brain (Fig.4f). Indeed, repeating the analysis after filtering out the sweeps from the activity traces significantly increases the correlation (Fig.S5a). In *SIFa* mutants, SIFa neurons also lose their activity cycles (Fig.4b,c); active and silent phases are replaced by an apparently unstructured train of sweeps. In this genetic background, the correlation between SIFa neuron activity and brainwide PSINA is dramatically reduced (Fig.4g), which at first suggested that SIFa neurons may be operating independently of the brainwide activity template. To our surprise, this correlation also increased significantly when we filtered out the sweeps (Fig.S5a), indicating that SIFa neuron activity is coupled to brainwide PSINA even in the absence of SIFa signaling.

We next recorded from SIFa neurons in *SIFaR* mutants. As the fluorescent marker associated with the $SIFaR^{null}$ allele overwhelmed the GCaMP6s signal from the four SIFa neurons, we carried out these experiments in the $SIFaR^{LoF}$ homozygous background (Fig.S5c-g). We found that SIFa neuron activity has disrupted cycles and reduced correlation to brainwide PSINA in the receptor mutants (Fig.S5c-e); these effects are directionally aligned with the *SIFa* mutant phenotypes but of lower magnitude, consistent with the weaker LoF receptor alleles. Despite the broad expression of *SIFaR* during PSINA (Fig.S3), two lines of evidence suggested that the SIFa neurons influence their own activity through autocrine signaling. First, before the onset of PSINA, SIFa neurons are labeled by the $SIFaR^{G4}$ gene trap (Fig.S3). Secondly, $SIFa^{G4}$-driven *SIFaR* knockdown alters brainwide PSINA (Fig.2f,g, Fig.S2d). However, we found that *SIFaR* expression in SIFa neurons alone does not restore wildtype activity to the SIFa neurons or to the rest of the brain (Fig.S5c,f-h). We conclude that *SIFaR* in SIFa neurons is necessary but not sufficient for wildtype autonomous or brainwide developmental activity.

The leading activity cycles of SIFa neurons suggested that these neurons are patterning brainwide PSINA. To test this in a gain-of-function context, we used the thermogenic cation channel TrpA1[31] to activate SIFa neurons. In our hands, both baseline and change in fluorescence recorded from GCaMP6s varies inversely with temperature. Consistent with this, SIFa neurons in control animals without TrpA1 moved to a lower baseline when shifted from 22 to 29°C, and, following a pause of ~1hr, resumed periodic activity cycles, albeit at a lower signal amplitude (Fig.4h). By contrast, TrpA1-expressing SIFa neurons responded to the temperature up-shift with a graded fluorescence increase which built up until the down-shift back to 22°C. In some cases, our recordings were clear enough to reveal more frequent activity cycles of lower amplitude on top of this graded response (Fig.4h:*Inset*). When carried out at ~70hAPF, brainwide PSINA response to SIFa neuron activation was stark (Fig.4i-k): on average, cycle frequency increased by ~80% (Fig.4j), resulting in a corresponding reduction in the period of ~40% (Fig.4k). This re-organization was achieved by running more, marginally shorter active phases at a higher duty cycle (i.e., shorter silent phases) and did not significantly alter the total signal compared to controls (Fig.4k). Activating SIFa neurons at ~80hAPF (Fig.S6), after their lead on the brain had shrunk considerably (Fig.4), did not alter the cycle frequency, but did reduce the silent phase duration as reported by the increased duty cycle. We did not observe any significant changes to brainwide PSINA when SIFa neurons were activated in *SIFa* mutants (Fig.4i,j, Fig.S6b,c). We conclude that SIFa neurons pattern PSINA cycles through SIFa-SIFaR signaling.

The only other gene we know to have a specific effect on the cycle period is the phospholipase C *NorpA*[6]: The period in *norpA* nulls is significantly longer, ranging from 200 to 125% of controls between 65-90hAPF (Fig.S7a,b). Specific expression of *UAS-NorpA* in SIFa neurons during pupal development fully restores the cycle period (Fig.S7b,c), indicating that this intracellular signaling factor is important for the proposed patterning role of SIFa neurons.

SIFa neurons pattern PSINA by modulating *Trpγ*+ neurons

We studied how *SIFa* interacts genetically with *Trpγ*. During pupal development, *Trpγ* is expressed in ~2,000 neurons, including the SIFa set[20]. Activating *Trpγ*+ neurons generates a continuous train of sweeps[20] while silencing the CB sub-population nearly eliminates brainwide PSINA (Fig.3 and [20]). Loss of *trpγ* gene function leads to distinctive changes in PSINA (Fig.5a-c): Average signal is reduced and the individual sweeps become shorter and more frequent (Fig.5b). In the wildtype, the regularity of activity cycles is diminished from 75hAPF on; this transition between the so-called periodic to the turbulent phases of PSINA[6] manifests as a blurring in the

main PSD band (Fig.5c). In *trpγ* mutants, active phases start to get longer around this time, leading to the appearance of a new, lower frequency band in the PSD (Fig.5c).

Comparison of single and double mutants revealed that *SIFa* and *Trpγ* have additive-multiplicative effects on brainwide PSINA. Average signal is reduced in double mutants beyond what we see for each single mutant; the double mutant signal profile across development is remarkably similar to the scaled product of the single mutant profiles (Fig.5b). A comparable effect is seen with sweeps: the single mutants of *trpγ* or *SIFa* gain or lose sweeps, respectively, and the double mutant phenotype is well-matched by the scaled product of the single mutant profiles (Fig.5b). Loss of both *SIFa* and *Trpγ* eliminates PSINA cycles in favor of a much slower undulation of ~1hr period. Notably, this low frequency band is present in all genetic backgrounds (Fig.5a,S8a), running at a shorter period of ~45 minutes in control and single mutant animals. Thus, compromising the high and medium frequency components of PSINA (i.e., sweeps and cycles) revealed a new low frequency component which we term *swells*. While we do not know the source of swells, the period increase in double mutants (Fig.S8a) is consistent with SIFa neurons, the only cells known to express both genes, playing a role in regulating this new feature of PSINA. These results show that *SIFa* and *Trpγ* make distinct but interdependent contributions to shaping brainwide PSINA.

The same genetic analysis for SIFa neuron activity shows that, in this single cell-type context, *SIFa* is epistatic to *Trpγ* (Fig.S8b-d). Neither the average signal nor sweep counts are significantly affected in single or double mutant animals (Fig.S8c). Instead, the phenotypes arise from how the activity is organized in time (Fig.S8b,d). In *trpγ* mutants, SIFa neurons retain their characteristic cycles; these gradually lengthen over time, recapitulating the brainwide *trpγ* phenotype and resulting in the appearance of the same lower frequency band in the PSD (Fig.S8d,5c). By contrast, cycles are altogether lost in both *SIFa* single and *SIFa*,*trpγ* double mutants. The main distinction between these genotypes is the longer swell period in the double mutants (Fig.S8b,e), paralleling the effect on brainwide PSINA (Fig.S8a).

In the crab stomatogastric ganglion, application of Gly1-SIFamide reorganizes a high frequency rhythm into a periodic bursting pattern[32]. Assuming SIFa-SIFaR signaling patterns PSINA cycles in analogous fashion, we can derive a mechanistic interpretation from the genetic analyses (see *Discussion*) with two additional observations. First, SIFa neuron *trpγ* phenotypes are non-cell-autonomous: Knockdown of *Trpγ* with $SIFa^{G4}$ leads to modest changes in brainwide PSINA, marginally decreasing signal and reducing the regularity of cycles (Fig.S9a-c). Consistent with this, *Trpγ* expression in SIFa neurons alone fails to rescue brainwide PSINA or SIFa neuron activity in *trpγ* mutants (Fig.S9d,e). By contrast, $Trp\gamma^{G4}$, a gene trap driver which captures the full functional expression domain of the gene[20,33], effectively rescues both activity profiles (Fig.S9d,e). These results suggest that the remarkably similar *trpγ* phenotypes in brainwide PSINA and SIFa neurons (Fig.5c,S8d) are largely due to loss of channel function in non-SIFa *Trpγ*+, or *Trpγ*± neurons. This inferred feedback from *Trpγ*± onto SIFa neurons is also consistent with the coupling between brainwide PSINA and SIFa neurons in *SIFa* mutants (Fig.S5a,b).

The second observation closes the circle: It is *SIFaR* expression in *Trpγ*+ neurons that allows for the patterning of cycles. Following up on the result that *SIFaR* expression is necessary in *Trpγ*+ neurons (Fig.2f,g), we found that $Trp\gamma^{G4}$ driven *UAS-SIFaR* largely rescues the *SIFaR* mutant phenotype (Fig.S10a-c). The *Trpγ-SIFaR* functional intersection also holds up under reciprocal necessity and sufficiency tests: Knockdown of *Trpγ* with the $SIFaR^{G4}$ significantly alters PSINA, including the signature extension of active phases (Fig.S9a-c). In addition, expression of *UAS-Trpγ* by $SIFaR^{G4}$ leads to near complete rescue of PSINA in *trpγ* mutants (Fig.S10d-f). Together, these results predicted that disruption of *Trpγ*+ neuron activity underlies the changes to brainwide PSINA seen in *SIFa* mutants. This is what we observed using two-channel imaging: In *SIFa* mutants, *Trpγ*+ neurons exhibit the same activity phenotypes we described for brainwide PSINA, and the two signals are highly correlated (Fig.5d-f). We conclude that SIFa neurons pattern the cycles of PSINA by modulating the activity of *Trpγ*+ neurons through SIFa-SIFaR signaling (Fig.5g).

DISCUSSION

We report that the neuropeptide gene *SIFa* and its receptor *SIFaR* are required in the developing central brain to establish the characteristic activity cycles of PSINA (Fig.1-3). SIFa neurons themselves have cycles which initiate before brainwide activity (Fig.4). Consistent with this implied causal role, activating SIFa neurons increases the frequency of brainwide cycles (Fig.4). Additionally, restoring NorpA function to just these four cells rescues the reduction in cycle frequency seen in *norpA* mutants (Fig.S7). Loss of *SIFa* or *SIFaR* gene function in SIFa neurons disrupts their activity (Fig.1,4,S5) indicating autocrine regulation. Wildtype SIFa neuron activity requires additional inputs, most notably from *Trpγ*± neurons (Fig.S9e). In turn, and consistent with the interaction

of the eponymous genes, SIFa neurons pattern the cycles of brainwide PSINA by modulating the activity of *Trpγ*± neurons (Fig.5).

The PSINA Engine

These results build on previous work[20] and allow us to propose a model of the core *PSINA engine*: a set of genetically-defined neural circuits in the central brain which establish the patterns of brainwide developmental activity (Fig.5g). In the absence of SIFa-SIFaR signaling, both SIFa neurons and brainwide PSINA or, equivalently, *Trpγ*± neurons lack cycles. They still remain coupled at the unmodulated rhythm of *Trpγ*± activity (Fig.S5a,b). This, and the similarity of the *SIFa* mutant and SIFa neuron silencing phenotypes (Fig.1e,2d), is consistent with *Trpγ*± neurons driving the coupling. The framework for superposing neuropeptide signaling onto these coupled oscillators is provided by the wealth of studies in the crustacean stomatogastric nervous system. In the crab, *Cancer borealis*, Gly1-SIFamide re-organizes the rhythms of the two interdependent central pattern generators driving food intake and processing[34]. Specifically, one defined neuronal type within these circuits responds to SIFa by increasing its high frequency rhythm and adding a low frequency bursting pattern[32]. Similarly, *Trpγ*± neurons gain more sweeps and both *Trpγ*± and SIFa neurons re-organize their activities into cycles in response to SIFa.

The PSINA engine can be further refined when informed by the developmental increase in SIFaR expression (Fig.S3) and the assumption that neuronal activity leads to SIFaR receptor inactivation (Fig.5g). In this model, SIFaR expression is limiting in *Trpγ*± neurons during the periodic phase of PSINA (55-75hAPF). This accounts for the longer SIFa neuron cycles which fully envelope brainwide activity (Fig.4b,e): At the front end, *Trpγ*± are slow to respond, and, at the back end, having expended their limited supply of SIFaR, they terminate cycles before the SIFa neurons. Over time, and in line with the increase in SIFaR expression, this envelope shrinks until, by 80hAPF, the SIFa neuron lead and lag is reduced to a few seconds. The extended brainwide cycles caused by SIFaR overexpression (Fig.S4b-d) are consistent with this mechanism. Loss of *Trpγ* (Fig.5c) also leads to extension of cycles at the transition out of the periodic phase (75-80hAPF); the reduced activity levels in this mutant background may increase the duration of SIFaR activity, sustaining the cycles for longer. Notably, SIFa neurons in *Trpγ* mutants have the same extended cycles (Fig.S8d), and $Trp\gamma^{G4}$, but not $SIFa^{G4}$, driven *UAS-Trpγ* expression can rescue this phenotype (Fig.S9e). We propose that, in the wildtype, *Trpγ*± neurons are feeding back onto the SIFa neurons to extend the duration of their autonomously periodic cycles, thereby transitioning the whole brain into the turbulent phase of PSINA. This feedback mechanism is also consistent with the more modest effect of activating SIFa neurons past 80hAPF (Fig.S6).

Wireless regulation of developmental activity

Neuropeptides are one of the largest and possibly the oldest class of neuro-active compounds[35,36]. Bilaterian genomes contain many dozens to over 100 neuropeptide genes; this diversity, along with a similar complement of GPCRs, underscores the neurophysiological potential of the chemical connectome[37–39]. In the developing brain, neuropeptides have been implicated in neurogenesis, morphogenesis, migration, survival, and circuit assembly[40–42]. While predicted[43], a direct involvement of neuropeptide signaling in developmental activity had not been demonstrated until the present study.

A defining feature of neuropeptide signaling is extra-synaptic volume transmission. This mode of communication frees neuropeptidergic cells from the constraints of specific post-synaptic contacts, giving them the reach and flexibility to integrate internal and external stimuli to regulate virtually every physiological and behavioral process in the adult[35,44–46]. During development, the same synapse-free access to neuromodulation would allow neuropeptide signaling to persist through on-going synaptogenesis, resolving the conceptual tension borne by developmental activity as a process tasked with refining synaptic connections it depends on. The possible precedence of neuropeptide signaling in developmental activity also aligns, in ontogeny recapitulates phylogeny fashion, with the chemical brain hypothesis[47]. According to this view, neuropeptide signaling, which may predate metazoan origins[48], organized the earliest neural networks prior to the emergence of synaptic transmission, after which neuropeptides took on the more familiar modulatory role.

Activity in the developing mammalian brain has been studied in discrete regions, and, in some cases, circuits or mechanisms which serve as local pattern generators have been identified[1]. How these distinct, local activity profiles are coordinated to mediate circuit integration[49] across disparate areas of the brain is not known. In the much smaller fly system, we show that cross brain coordination is driven by a central pattern generator and relay circuit, the PSINA engine, which minimally comprises the SIFa and *Trpγ*± neurons. Notably, silencing the central PSINA engine reveals local oscillators in the optic lobes (Fig.3c), suggesting that even at the scale of the fly, global coordination of developmental activity is a built-in feature. SIFa neurons reside in the PI, the neuropeptide

335 and hormone center of the fly brain, and functional homolog of the mammalian hypothalamus. It was recently reported that hypothalamic peptidergic neurons project into nearly all areas of the mouse brain[50], confirming that the mammalian nervous system has the infrastructure to mediate long-range neuropeptide-mediated coordination; it remains to be seen whether this infrastructure is used during development.

Altering developmental activity is expected to affect behavior, and changes to spontaneous network activity 340 in the developing mammalian cortex are thought to be linked to neurodevelopmental disorders[2]. In the fly, disruption of SIFa-SIFaR signaling affects a range of behaviors; whether these phenotypes are due to loss of neuropeptide signaling in the adult or during development is a matter of interest[51]. The advantages of the fly and our improving handle on the PSINA engine will make it possible to address how PSINA contributes to the emergence neurotypical behavior.

345

ACKNOWLEDGEMENTS

We thank J. M. Donlea, M. A. Frye, E. Marcus, S. L. Zipursky, and members of the Akin Lab for discussions, support and feedback on the manuscript; J. A. Veenstra for sharing SIFa antibodies; D. Hattori for the KiR2.1 flies; A. Nern and G. M. Rubin for the 29C07-FLP flies; B. Deng and Y. Rao for the SIFa[attP] flies; and C. G. 350 Vecsey for a number of fly lines. OA is supported by NIH grant R01NS123376 and W. M. Keck Foundation Junior Faculty Award.

REFERENCES

1. Blankenship, A. G. & Feller, M. B. Mechanisms underlying spontaneous patterned activity in developing neural circuits. *Nature Reviews Neuroscience* **11**, 18–29 (2010).
2. Wu, M. W., Kourdougli, N. & Portera-Cailliau, C. Network state transitions during cortical development. *Nat. Rev. Neurosci.* **25**, 535–552 (2024).
3. Martini, F. J., Guillamón-Vivancos, T., Moreno-Juan, V., Valdeolmillos, M. & López-Bendito, G. Spontaneous activity in developing thalamic and cortical sensory networks. *Neuron* **109**, 2519–2534 (2021).
4. Akin, O. & Zipursky, S. L. Activity regulates brain development in the fly. *Current Opinion in Genetics & Development* **65**, 8–13 (2020).
5. Willshaw, D. J., Von Der Malsburg, C. & Longuet-Higgins, H. C. How patterned neural connections can be set up by self-organization. *Proceedings of the Royal Society of London. Series B. Biological Sciences* **194**, 431–445 (1976).
6. Akin, O., Bajar, B. T., Keles, M. F., Frye, M. A. & Zipursky, S. L. Cell-type-Specific Patterned Stimulus-Independent Neuronal Activity in the Drosophila Visual System during Synapse Formation. *Neuron* **101**, 894-904.e5 (2019).
7. Terhzaz, S., Rosay, P., Goodwin, S. F. & Veenstra, J. A. The neuropeptide SIFamide modulates sexual behavior in Drosophila. *Biochemical and Biophysical Research Communications* **352**, 305–310 (2007).
8. Jørgensen, L. M., Hauser, F., Cazzamali, G., Williamson, M. & Grimmelikhuijzen, C. J. P. Molecular identification of the first SIFamide receptor. *Biochemical and Biophysical Research Communications* **340**, 696–701 (2006).
9. Hevesi, Z., Hökfelt, T. & Harkany, T. Neuropeptides: The Evergreen Jack-of-All-Trades in Neuronal Circuit Development and Regulation. *BioEssays* **47**, e202400238 (2025).
10. Thompson, A., Gribizis, A., Chen, C. & Crair, M. C. Activity-dependent development of visual receptive fields. *Current Opinion in Neurobiology* **42**, 136–143 (2017).
11. Kersbergen, C. J., Babola, T. A., Rock, J. & Bergles, D. E. Developmental spontaneous activity promotes formation of sensory domains, frequency tuning and proper gain in central auditory circuits. *Cell Reports* **41**, 111649 (2022).
12. Antón-Bolaños, N. *et al.* Prenatal activity from thalamic neurons governs the emergence of functional cortical maps in mice. *Science* **364**, 987–990 (2019).
13. Ge, X. *et al.* Retinal waves prime visual motion detection by simulating future optic flow. *Science* **373**, (2021).
14. Tiriac, A., Bistrong, K., Pitcher, M. N., Tworig, J. M. & Feller, M. B. The influence of spontaneous and visual activity on the development of direction selectivity maps in mouse retina. *Cell Reports* **38**, 110225 (2022).
15. Matsumoto, N., Barson, D., Liang, L. & Crair, M. C. Hebbian instruction of axonal connectivity by endogenous correlated spontaneous activity. *Science* **385**, eadh7814 (2024).
16. Crair, M. C. Neuronal activity during development: permissive or instructive? *Current Opinion in Neurobiology* **9**, 88–93 (1999).
17. Carreira-Rosario, A., York, R. A., Choi, M., Doe, C. Q. & Clandinin, T. R. Mechanosensory input during circuit formation shapes Drosophila motor behavior through patterned spontaneous network activity. *Current biology : CB* (2021) doi:10.1016/j.cub.2021.08.022.
18. Chen, Y. *et al.* Cell-type-specific labeling of synapses in vivo through synaptic tagging with recombination. *Neuron* **81**, 280–293 (2014).
19. Muthukumar, A. K., Stork, T. & Freeman, M. R. Activity-dependent regulation of astrocyte GAT levels during synaptogenesis. *Nature Neuroscience* **17**, 1340–1350 (2014).
20. Bajar, B. T. *et al.* A discrete neuronal population coordinates brain-wide developmental activity. *Nature* **602**, 639–646 (2022).
21. Verleyen, P. *et al.* SIFamide is a highly conserved neuropeptide: a comparative study in different insect species. *Biochemical and Biophysical Research Communications* **320**, 334–341 (2004).
22. Wolff, T. *et al.* Cell type-specific driver lines targeting the Drosophila central complex and their use to investigate neuropeptide expression and sleep regulation. *eLife* **14**, (2025).
23. Namiki, S., Dickinson, M. H., Wong, A. M., Korff, W. & Card, G. M. The functional organization of descending sensory-motor pathways in Drosophila. *eLife* **7**, e10806 (2018).
24. Martelli, C. *et al.* SIFamide Translates Hunger Signals into Appetitive and Feeding Behavior in Drosophila. *CellReports* **20**, 464–478 (2017).
25. Dreyer, A. P. *et al.* A circadian output center controlling feeding:fasting rhythms in Drosophila. *PLOS Genetics* **15**, e1008478 (2019).

26. Bai, L. *et al.* A Conserved Circadian Function for the Neurofibromatosis 1 Gene. *CellReports* **22**, 3416–3426 (2018).
27. Park, S., Sonn, J. Y., Oh, Y., Lim, C. & Choe, J. SIFamide and SIFamide receptor defines a novel neuropeptide signaling to promote sleep in Drosophila. *Molecules and cells* **37**, 295–301 (2014).
28. Sellami, A. & Veenstra, J. A. SIFamide acts on fruitless neurons to modulate sexual behavior in Drosophila melanogaster. *Peptides* **74**, 50–56 (2015).
29. Nässel, D. R. Substrates for Neuronal Cotransmission With Neuropeptides and Small Molecule Neurotransmitters in Drosophila. *Frontiers in Cellular Neuroscience* **12**, 83 (2018).
30. Aso, Y. *et al.* The neuronal architecture of the mushroom body provides a logic for associative learning. *eLife* **3**, e04577 (2014).
31. Pulver, S. R., Pashkovski, S. L., Hornstein, N. J., Garrity, P. A. & Griffith, L. C. Temporal dynamics of neuronal activation by Channelrhodopsin-2 and TRPA1 determine behavioral output in Drosophila larvae. *Journal of Neurophysiology* **101**, 3075–3088 (2009).
32. Fahoum, S.-R. H. & Blitz, D. M. Neuronal Switching between Single- and Dual-Network Activity via Modulation of Intrinsic Membrane Properties. *J. Neurosci.* **41**, 7848–7863 (2021).
33. Akitake, B. *et al.* Coordination and fine motor control depend on Drosophila TRPγ. *Nature communications* **6**, 7288 (2015).
34. Blitz, D. M., Christie, A. E., Cook, A. P., Dickinson, P. S. & Nusbaum, M. P. Similarities and differences in circuit responses to applied Gly1-SIFamide and peptidergic (Gly1-SIFamide) neuron stimulation. *Journal of Neurophysiology* **121**, 950–972 (2019).
35. Beets, I. & Watteyne, J. Mapping and decoding neuropeptide signaling networks in nervous system function. *Current Opinion in Neurobiology* **92**, 103027 (2025).
36. Hauser, F., Koch, T. L. & Grimmelikhuijzen, C. J. P. Review: The evolution of peptidergic signaling in Cnidaria and Placozoa, including a comparison with Bilateria. *Front. Endocrinol.* **13**, (2022).
37. Ripoll-Sánchez, L. *et al.* The neuropeptidergic connectome of C. elegans. *Neuron* **111**, 3570-3589.e5 (2023).
38. Deng, B. *et al.* Chemoconnectomics: Mapping Chemical Transmission in Drosophila. *Neuron* **101**, 876-893.e4 (2019).
39. Smith, S. J. *et al.* Single-cell transcriptomic evidence for dense intracortical neuropeptide networks. *eLife* **8**, e47889 (2019).
40. Bakos, J., Zatkova, M., Bacova, Z. & Ostatnikova, D. The Role of Hypothalamic Neuropeptides in Neurogenesis and Neuritogenesis. *Neural Plasticity* **2016**, 3276383 (2016).
41. Li, Z.-H., Li, B., Zhang, X.-Y. & Zhu, J.-N. Neuropeptides and Their Roles in the Cerebellum. *International Journal of Molecular Sciences* **25**, 2332 (2024).
42. Hevesi, Z. *et al.* Transient expression of the neuropeptide galanin modulates peripheral-to-central connectivity in the somatosensory thalamus during whisker development in mice. *Nat Commun* **15**, 2762 (2024).
43. Hevesi, Z., Hökfelt, T. & Harkany, T. Neuropeptides: The Evergreen Jack-of-All-Trades in Neuronal Circuit Development and Regulation. *BioEssays* **47**, e202400238 (2025).
44. Jékely, G. & Yuste, R. Nonsynaptic encoding of behavior by neuropeptides. *Current Opinion in Behavioral Sciences* **60**, 101456 (2024).
45. Nässel, D. R. & Zandawala, M. Recent advances in neuropeptide signaling in *Drosophila*, from genes to physiology and behavior. *Progress in Neurobiology* **179**, 101607 (2019).
46. Nässel, D. R. & Zandawala, M. Endocrine cybernetics: neuropeptides as molecular switches in behavioural decisions. *Open Biology* **12**, 220174 (2022).
47. Jékely, G. The chemical brain hypothesis for the origin of nervous systems. *Philosophical Transactions of the Royal Society B: Biological Sciences* **376**, 20190761 (2021).
48. Yañez-Guerra, L. A., Thiel, D. & Jékely, G. Premetazoan Origin of Neuropeptide Signaling. *Molecular Biology and Evolution* **39**, msac051 (2022).
49. Guillamón-Vivancos, T. *et al.* Input-dependent segregation of visual and somatosensory circuits in the mouse superior colliculus. *Science* **377**, 845–850 (2022).
50. Jiao, Z. *et al.* Projectome-based characterization of hypothalamic peptidergic neurons in male mice. *Nat Neurosci* 1–16 (2025) doi:10.1038/s41593-025-01919-0.
51. Huang, H., Possidente, D. R. & Vecsey, C. G. Optogenetic activation of SIFamide (SIFa) neurons induces a complex sleep-promoting effect in the fruit fly Drosophila melanogaster. *Physiology & Behavior* **239**, 113507 (2021).

52. Bainbridge, S. P. & Bownes, M. Staging the metamorphosis of Drosophila melanogaster. *Journal of embryology and experimental morphology* **66**, 57–80 (1981).
53. Brand, A. H. & Perrimon, N. Targeted gene expression as a means of altering cell fates and generating dominant phenotypes. *Development* **118**, 401–415 (1993).
54. Lai, S.-L. & Lee, T. Genetic mosaic with dual binary transcriptional systems in Drosophila. *Nature Neuroscience* **9**, 703–709 (2006).
55. Schindelin, J. *et al.* Fiji: an open-source platform for biological-image analysis. *Nat Methods* **9**, 676–682 (2012).
56. Uhlén, P. Spectral Analysis of Calcium Oscillations. *Sci. STKE* **2004**, (2004).
57. Nern, A., Pfeiffer, B. D. & Rubin, G. M. Optimized tools for multicolor stochastic labeling reveal diverse stereotyped cell arrangements in the fly visual system. *Proceedings of the National Academy of Sciences* **112**, E2967–E2976 (2015).

METHODS

Experimental model and subject details

Flies were reared at 18°C, 25°C, or 29°C on standard cornmeal/molasses medium; developmental time was matched to the 25°C standard (1x) using relative rates of 0.5x and 1.25x for 18°C and 29°C[52], respectively. Pupal development was staged relative to white pre-pupa formation (w.p.p., 0hAPF) or head eversion (h.e., 12hAPF). GAL4/UAS[53] and LexA/LexAop[54] expression systems were used to drive cell-type-specific transgene expression. The available molecularly-defined null allele of *SIFaR*, *SIFaR*$^{[attP]}$[38], appeared to be homozygous lethal. However, complementation tests indicated that a second site mutation was the cause of the lethality, and we recovered a viable SIFaR$^{[attP]}$ line through out-crosses. Complete genotypes used in each experiment can be found in Supplementary Table 1.

Widefield imaging

Bottle-scale (~100 virgins, 10-20 males) crosses were setup for each genotype of each experimental set and reared at 18°C-29°C depending on experimental design. Pupae were genotyped and staged at w.p.p. or h.e. All data shown were collected from female pupae; mutant phenotypes of *SIFa* and *SIFaR* (Fig.1) were also confirmed in males (not shown). Imaging sessions typically started ~50hAPF and lasted until eclosion (~100hAPF). To prepare the pupae for imaging, the cuticle around the head was removed with fine forceps and the animals were fixed to a metal plate (McMaster-Carr) with double-sided adhesive tape (3M). The metal plate was placed in a custom environmental chamber to maintain temperature and humidity. This chamber comprised: a PTC1 temperature-controlled breadboard (Thorlabs) to maintain sample temperature at a designated set-point; a set of four 35-mm dishes filled with deionized water to maintain humidity; and a 150-mm petri-dish lid to provide enclosure. To improve imaging quality, a large format coverslip was fitted into a rectangular opening made in the lid. This coverslip sat in the optical path, between the pupae and the objective lens, and was treated with Barbasol shaving cream (Perio) to prevent condensation during temperature shifts.

Images were acquired using either a Zeiss (1- and 2-channel imaging) Axio Zoom.V16 epifluorescence microscope equipped with a Retiga R1 CCD Camera (QImaging) and X-Cite TURBO 6-Channel LED Light Source (Excelitas Technologies), or a Leica (1-channel imaging) M165FC epifluorescence microscope with a Leica.K5 Camera and CoolLED 3-Channel Light Source (CoolLED). Images were acquired at 0.5 Hz with 100ms exposure time for GCaMP6s and 200ms exposure time for jRCaMP1b (5-20mW under objective power). Acquisition was controlled by Slidebook software (Intelligent Imaging Innovations) on the Zeiss microscope and LAS X (Leica Inc) on the Leica microscope. Time series were processed with Fiji[55](ImageJ) and analyzed using MATLAB (Mathworks); see below.

Immunofluorescence and confocal microscopy

Brains were dissected in cold Schneider Medium (Gibco 21720–024) and fixed with 4% v/v PFA (Electron Microscopy Sciences 15710) in Schneider Medium for 20 min at room temperature. Brains were then washed out of fixative into PBS (Quality Biological), solubilized in PBST (0.5% Triton-X100 (Sigma T9284) in PBS) for 1 h, and blocked in PBTN (5% Normal Donkey Serum (Jackson ImmunoResearch no. 017-000-121) in PBST) for 1-2 h, all at room temperature. Brains were sequentially incubated in primary and secondary antibodies diluted in PBTN for 24–48 h at 4 °C, with at least 3 washes through PBST over 2 h at room temperature in between and afterwards. Brains were post-fixed with 4% v/v PFA in Schneider Medium for 20 min at room temperature, followed by multiple washes into PBST over 10 min. Brains were finally transferred to Everbrite mounting medium (Biotium 23001) and mounted on to slides for imaging.

Primary antibodies and dilutions used in this study were as follows: chicken anti-GFP (Abcam ab13970, 1:1,000), mouse monoclonal anti-V5 (Novus Biologicals NBP2-52703–0.2 mg, 1:150), rat monoclonal anti-Ncad (DSHB DN-Ex 8-c, 1:100), mouse monoclonal anti-Brp (DSHB nc82-c, 1:150), and rabbit polyclonal anti-SIFamide[7] (1:1,000).

Secondary antibodies and dilutions used in this study were as follows: Alexa 488 donkey polyclonal anti-chicken (Jackson ImmunoResearch 703-545-155, 1:400), Alexa 488 donkey polyclonal anti-mouse (Jackson ImmunoResearch 715-545-151, 1:400), Alexa 488 donkey polyclonal anti-rabbit (Jackson ImmunoResearch 712-545-153, 1:400), Alexa 568 donkey polyclonal anti-mouse (Jackson ImmunoResearch 715-575-150, 1:400), Alexa 568 donkey polyclonal anti-rabbit (Invitrogen A10042, 1:400), Alexa 647 donkey polyclonal anti-rat (Jackson ImmunoResearch 712-605-153, 1:400), and Alexa 647 donkey polyclonal anti-rabbit (Jackson ImmunoResearch 711-605-152, 1:400)

Immunofluorescence images were acquired using a Zeiss LSM 780 confocal microscope with 20×/0.8 air, 40×/1.4 oil immersion or 40×/1.2 glycerol immersion objectives (Zeiss). Images were prepared for publication using Fiji[55](ImageJ).

535

Analysis of widefield imaging data

User-defined ROIs from time series were selected in Fiji[55] (ImageJ). Custom scripts written in MATLAB (Mathworks) were used in all subsequent analysis. Raw fluorescence traces from per frame ROI pixel averages (F) were fit to a baseline (F_0) and $\Delta F/F_0$ (signal) was calculated by subtracting the baseline from the raw signal
540 and dividing by the baseline. Between 75-85hAPF, the raw fluorescence recorded from intact pupae exhibits a stereotyped sigmoidal decrease in intensity correlated with the maturation of the cuticle around the head. By comparing this trend, captured by the baseline fit (F_0), to staged animals, we found that the inflection point of the curve corresponds to ~80hAPF. In all analyses, this internal, genotype-independent feature was used to synchronize the developmental ages of the animals. The pace of PSINA (e.g., cycle frequency) is temperature
545 sensitive. To compare data collected at different temperatures, we scaled the time axes of the recordings to match the 25°C standard (1x) using the coefficient $T_{Coef}=100/(-0.0465*T^3+4.263*T^2-133.49*T+1500)$, where T is the recording temperature in degrees Celsius. The formula is derived from the best fit third order polynomial to the measured temperature-dependent duration of metamorphosis[52]. Active phase limits were defined using a threshold set to 4% of average maximum signal recorded from control genotypes with a minimum floor of 0.5%
550 $\Delta F/F_0$ for low signal-to-noise data (e.g., SIFa neuron recordings).

PSDs were calculated for each hour of recording using a 2-h sliding window[56]. In preparation for Fast Fourier Transform and PSD estimation, each 2-h segment was filtered to isolate target frequencies (standard 120s Gaussian window to remove sweeps or defined low pass cutoffs as noted in Figure legends), centered on the time axis by subtracting its mean, and multiplied with the Hanning window function to reduce spectral leakage.
555 The PSD for each 2-hr segment was normalized relative to its discrete integral over all frequencies; this step effectively removes the contribution of signal amplitude changes to the PSD in order to focus on frequency changes for subsequent comparisons. Each experimental condition thus yielded a distribution of normalized PSD values (as many as replicate number) at each frequency-time coordinate. Statistical tests between different experimental conditions were carried out between these distributions. PSDs from all replicates of an
560 experimental condition were averaged to generate the average PSD panels shown in the Figures.

All statistical analyses were carried out using the non-parametric two-sample Kolmogorov-Smirnov test; p values less than 0.05 were considered significant.

FIGURE LEGENDS

Figure 1. *SIFa* and *SIFaR* are necessary for PSINA cycles

a. 65 hAPF *D. melanogaster* pupa. Cuticle around the head (boxed) has been removed for widefield imaging. Brain is outlined: CB, central brain; OL, optic lobe. Scale bar, 500µm.

b. Montage of pupal heads from one widefield imaging session. Signal is fluorescence from pan-neuronally expressed GCaMP6s. Yellow rectangle (top-right) is typical region of interest (ROI) used to extract PSINA traces. All time axes in this and following figures are in units of hAPF. Scale bar, 500µm.

c. *Top:* Wildtype PSINA recorded from enumerated pupae in (b); sampling rate is 0.5Hz. *Bottom:* Expanded view of PSINA from the blue highlighted 1h span above depicting the active (ON) and silent (OFF) phases of activity cycles, sweeps, and principal metrics used in analyses. PSD, power spectral density: PSINA traces were filtered to remove sweeps (coral overlaid profile), and PSD was estimated using the Discrete Fourier Transform ('F').

d. Maximum intensity projection (MIP) of 72hAPF brain with *SIFaR*^{G4} driving *mCherry.NLS* (native fluorescence, cyan-hot look-up table (LUT)); brain also stained against SIFa (orange-hot LUT) and N-Cadherin (magenta). Green rectangle boxes SIFa soma. CB, central brain; OL, optic lobe; PI, Pars Intercerebralis. Scale bar, 100µm.

e-g. *SIFa* mutant analysis

e. Representative PSINA traces, color-matched to genotypes shown; numbers are sample sized used in (f) and (g). *Df*, deficiency; *Dp*, genomic duplication.

f. Duty cycle and average signal, normalized to control genotype (black). Inset in duty cycle plots true values of metric. Shaded areas, standard deviation. Closed circles mark where experimental distribution differs from control ($p<0.05$) by two-sample KS test.

g. Average PSDs from control (first column) and experimental (second column) animals. PSD for each PSINA trace was calculated at every hour within a 2h sliding window and normalized to remove contribution from changes in signal amplitude. Displayed PSDs are averages of replicates for each condition. Labels color-matched to (e,f); sample sizes indicated. PSD comparison of *SIFa*$^{[1]}$/*SIFa*$^{[2]}$ to +/*SIFa*$^{[1]}$ omitted for brevity. In third column, bottom panel of each set maps p-values from KS tests of control and experimental PSD distributions at each frequency-time coordinate; $p<0.05$ displayed in magenta. Top panel is fraction of control signal power re-assigned to different ($p<0.05$) frequencies in the experimental data.

h-j. *SIFaR* mutant analysis with *SIFaR*^{LoF} (i.e., *SIFaR*^{GFSTF}); data presented as in (e-g).

Figure 2. *SIFa* and *SIFaR* are necessary during PSINA

a. Temperature schedule used to temporally target RNAi knockdown and KiR2.1 expression to pupal development.

b,c. Temporally-targeted knockdown of *SIFa*.

b. PSINA traces, color-matched to genotypes shown; numbers are sample sized used in (c).

c. Average PSDs from control and experimental animals; presented as in Fig.1g.

d,e. Temporally-targeted KiR2.1 expression in SIFa neurons; presented as in (b,c).

f,g. Temporally-targeted knockdown of *SIFaR*; presented as in (b,c).

h. Temporally-targeted SIFaR^{G4}-driven KiR2.1 expression; one control and three experimental traces shown.

Figure 3. SIFaR in the central brain is necessary for wildtype PSINA cycles

a. Spatial fractionation of GAL4 expression. Both schemes carry two variants of *tubP-GAL80*: *GAL80ts* and one of two FLP-responsive conditional alleles. In the optic lobes, OL-FLP (29C07-FLP^{57}) either turns on *GAL80* expression by removing the interruption cassette ('-STOP-', top) or turns it off by locally excising the FRT-flanked ORF (bottom). Animals are reared at 18°C and shifted 29°C at in the early pupa to unmask these differential *GAL80* expression domains ahead of PSINA onset; *GAL4*-driven effector expression is disinhibited in the complementary domains (blue). CB, central brain. OL, optic lobe.

b. Anterior-posterior (A/P) and dorso-ventral (D/V) MIPs of 60hAPF brains with *PanN*-, *Trpγ*-, or *SIFaR*-GAL4 driving *UAS-KiR2.1-T2A-tdTOM* expression principally in the CB (top row) or the OLs (bottom row). *PanN* labeling reveals some posterior OL neurons in the CB-designated fraction and Kenyon cells in the OL-designated fraction. KiR2.1 expression domain detected through tdTOM native fluorescence (cyan-hot LUT); reference stain is N-Cadherin (magenta). Scale bar, 100µm.

c,f. Representative PSINA traces from animals in which KiR2.1 (c) or SIFaR-RNAi (f) expression was targeted to the CB (top set) or OL (bottom set) with the indicated *GAL4*s. CB (left columns) or OL (right columns) recordings are from the same animal in each condition.

d,g. *Left*: Normalized average signal from animals in which KiR2.1 (d) or SIFaR-RNAi (g) expression was spatially targeted to the CB and recorded from the CB (top) or OL (bottom). Genotypes color-matched to (c) and (f); sample sizes indicated in *Right.* Closed circles mark where experimental distributions differ from control ($p<0.05$) by two-sample KS test.
Right: Average PSDs from control and experimental conditions described for *Left*; presented as in Fig.1g.
e,h. Data from animals in which KiR2.1 (e) or SIFaR-RNAi (h) expression was spatially targeted to the OLs; presentation as in (d,g).

Figure 4. SIFa neurons pattern brainwide PSINA
a-g. PSINA v. SIFa neuron activity in wildtype and *SIFa* mutant animals.
a. 2-channel recording of SIFa neuron activity (cyan) and brainwide PSINA (magenta). *Left:* Pan-neuronal>RCaMP and SIFa neuron>GCaMP overlay of pupal head at 69.5 hAPF. *Right:* Progressive frames from boxed span no.1 in (b). Color-matched ROIs from *left* shown; intensities adjusted to display fluorescence changes.
b. *Left:* Representative traces for the indicated conditions. PSINA, as reported by pan-neuronal RCaMP, was recorded from the SIFa neuron ROI. *Right:* Expanded views for numbered boxes in *left*; SIFa neuron active phases demarcated in light blue.
c. PSD comparison of SIFa neuron activity in control and *SIFa* mutant animals; sample sizes as indicated.
d. PSD comparison of PSINA, as reported by pan-neuronal RCaMP, and SIFa neuron activity in control (top) and *SIFa* mutant (bottom) animals; sample sizes as indicated.
e. Active phase rise time differences between SIFa neurons and central brain (blue) or left optic lobe and central brain (magenta). ~30 data points per hourly distribution compiled from 12 traces; shaded areas, s.d. Closed circles mark where the blue distributions differ from magenta ($p<0.05$) by two-sample KS test.
f. Zero-lag correlation of SIFa-ROI pan-neuronal activity to left optic lobe in control and *SIFa* mutant animals.
g. Zero-lag correlation of SIFa neuron to SIFa-ROI pan-neuronal activity in control and *SIFa* mutant animals.
h-k. TrpA1 activation of SIFa neurons
h. *Top:* Temperature schedule used. *Bottom:* SIFa neuron activity response to temperature shift, with (blue) and without (black) TrpA1. Dashed lines mark GCaMP6s baseline at 22°C. Inset expanded view of gray highlighted span.
i. Representative PSINA traces at 29°C for the indicated genotypes.
j. PSD comparison of PSINA at 29°C in control (top) and *SIFa* mutant (bottom) animals with and without TrpA1 expression in SIFa neurons; sample sizes as indicated.
k. PSINA metrics at 29°C for the indicated genotypes. Major period corresponds to the dominant frequency in the PSD. Shaded areas, s.d. Closed circles mark where experimental distributions (magenta) differ from control ($p<0.05$) by two-sample KS test.

Figure 5. SIFa neurons pattern PSINA by modulating *Trpγ+* neurons
a-c. Double mutant analysis of *SIFa* and *Trpγ.*
a. *Top*: Representative traces for the indicated genotypes shown below long-pass filtered ($<5.6\times10^{-4}$ Hz, >30 min) derivates (i.e., swells). *Bottom*: Expanded view of the gray highlighted span in *top*.
b. Average signal and sweeps per hour, both normalized to control, for the genotypes and sample sizes in (a). Magenta traces are scaled products of the single mutant average values. Shaded areas, s.d. Closed circles mark where experimental distributions differ from control ($p<0.05$) by two-sample KS test.
c. Average PSDs from control and experimental animals; presented as in Fig.1g.
d-f. PSINA v. *Trpγ+* neuron activity in wildtype and *SIFa* mutant animals.
d. Representative traces from 2-channel recordings of *Trpγ+* neuron activity and brainwide PSINA in control and *SIFa* mutant animals.
e. Zero-lag correlation of *Trpγ+* neuron activity to brainwide PSINA in control and *SIFa* mutant animals.
f. PSD comparison of *Trpγ+* neuron activity and PSINA in control (top) and *SIFa* mutant (bottom) animals; sample sizes as indicated.
g. Model of the core PSINA engine. In the absence SIFa signaling (left, 'No SIFa'), neither SIFa (blue) nor *Trpγ±* (magenta) neurons have stereotyped cycles; however, the activity profiles remain coupled due to input from *Trpγ±* neurons. SIFa-SIFaR signaling patterns both activity profiles into cycles (right, 'With SIFa'), and brainwide PSINA follows the *Trpγ±* neuron activity template. SIFaR expression (light gray gradient ramp) and activity levels (dark gray triangles) control for how long *Trpγ±* neurons can sustain an active phase. See *Discussion* for more details.

Figure 1

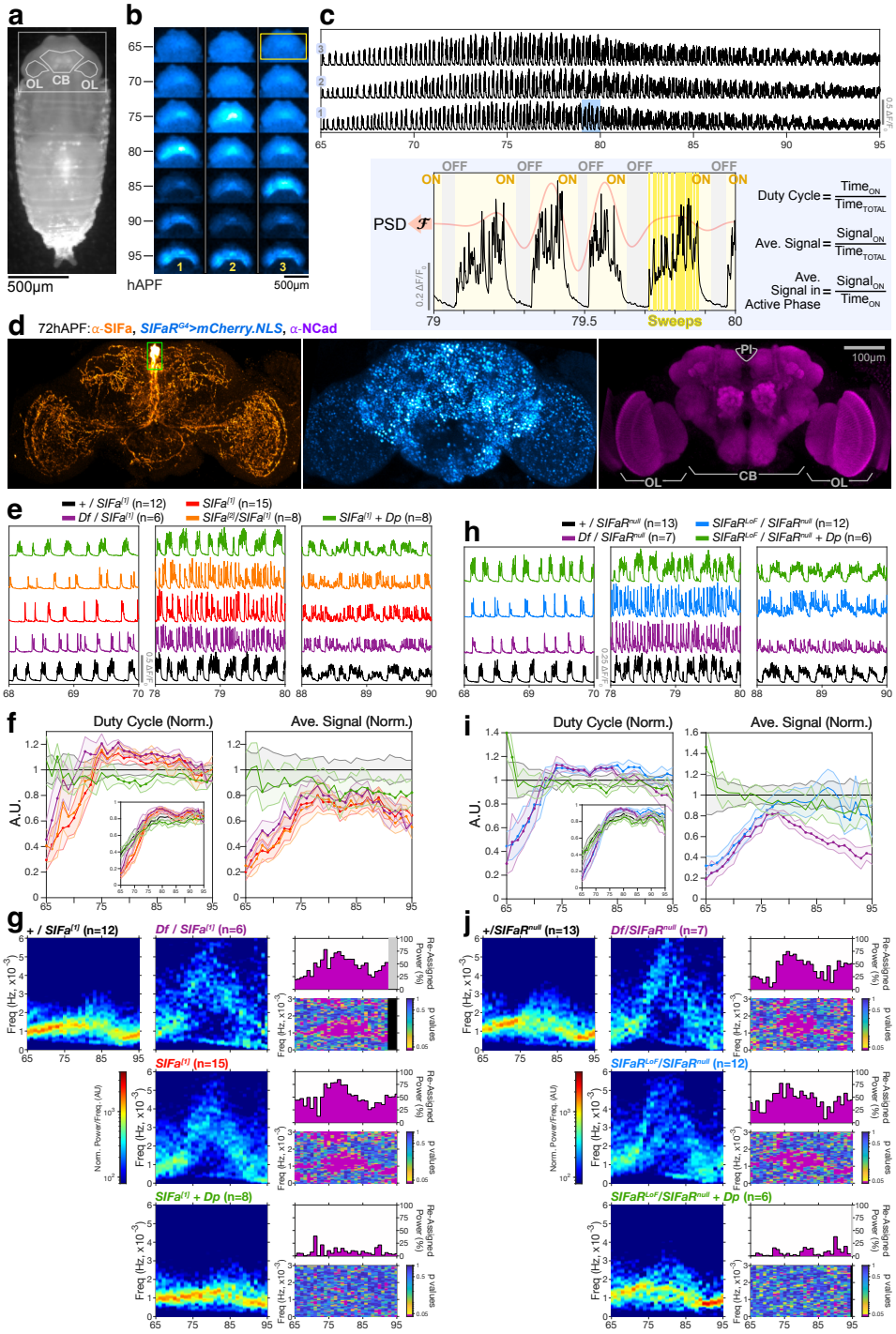
a
OL
CB
OL
500µm
b
hAPF
500µm
c
PSD
OFF
ON
Duty Cycle = Time_ON / Time_TOTAL
Ave. Signal = Signal_ON / Time_TOTAL
Ave. Signal in Active Phase = Signal_ON / Time_ON
Sweeps
d
72hAPF: α-SIFa, SIFaR^G4>mCherry.NLS, α-NCad
PI
100µm
OL
CB
OL
e
+ / SIFa[1] (n=12)
SIFa[1] (n=15)
Df / SIFa[1] (n=6)
SIFa[2]/SIFa[1] (n=8)
SIFa[1] + Dp (n=8)
h
+ / SIFaR^null (n=13)
SIFaR^LoF / SIFaR^null (n=12)
Df / SIFaR^null (n=7)
SIFaR^LoF / SIFaR^null + Dp (n=6)
f
Duty Cycle (Norm.)
Ave. Signal (Norm.)
A.U.
i
Duty Cycle (Norm.)
Ave. Signal (Norm.)
A.U.
g
+ / SIFa[1] (n=12)
Df / SIFa[1] (n=6)
SIFa[1] (n=15)
SIFa[1] + Dp (n=8)
Freq (Hz, x10^-3)
Re-Assigned Power (%)
p values
Norm. Power/Freq. (AU)
j
+/SIFaR^null (n=13)
Df/SIFaR^null (n=7)
SIFaR^LoF/SIFaR^null (n=12)
SIFaR^LoF/SIFaR^null + Dp (n=6)

Figure 2

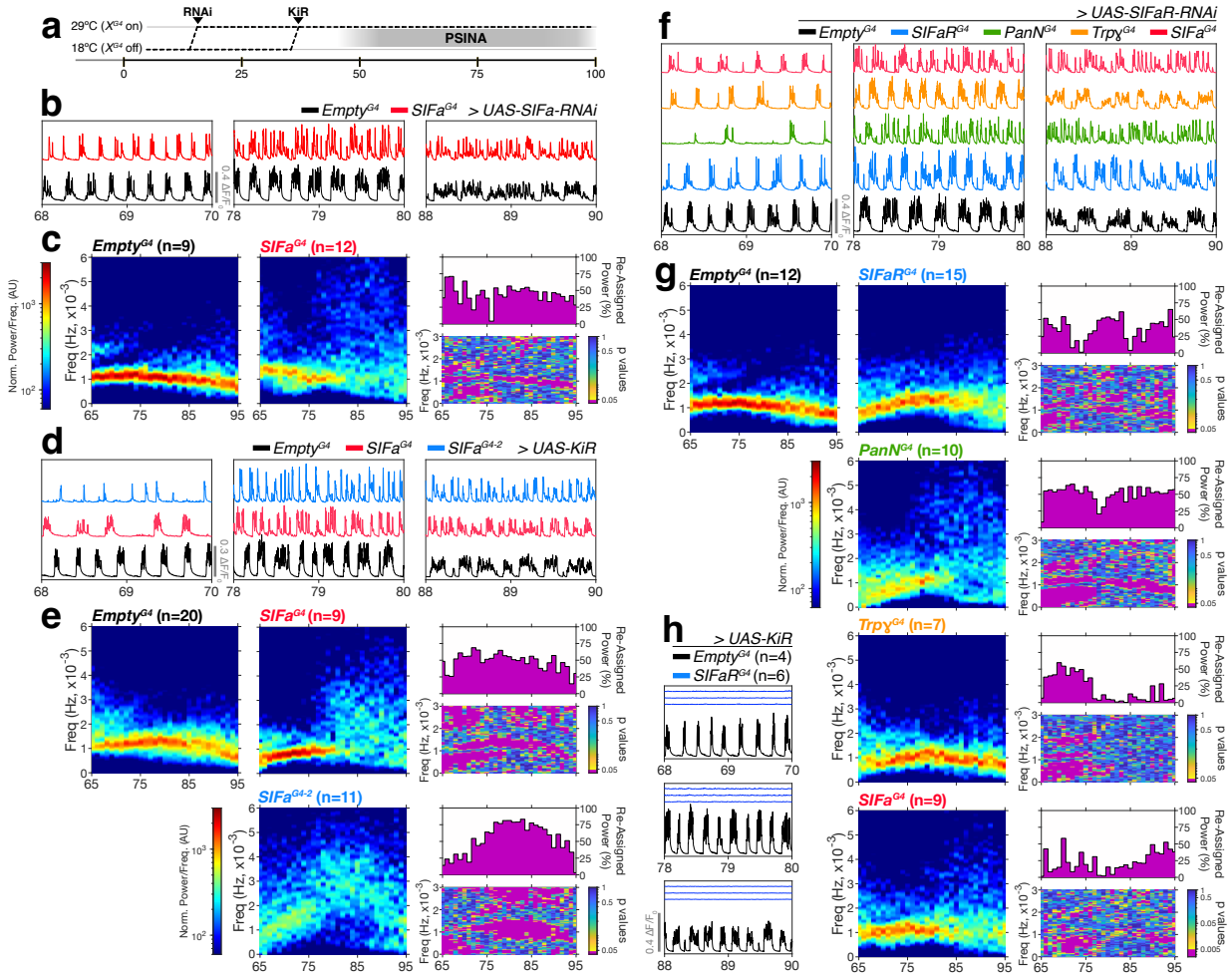
a
RNAi
KiR
29ºC (X^G4 on)
18ºC (X^G4 off)
PSINA
0
25
50
75
100
b
Empty^G4
SIFa^G4
> UAS-SIFa-RNAi
0.4 ΔF/F0
68
69
70
78
79
80
88
89
90
c
Empty^G4 (n=9)
SIFa^G4 (n=12)
Norm. Power/Freq. (AU)
Freq (Hz, x10^-3)
Re-Assigned Power (%)
p values
d
Empty^G4
SIFa^G4
SIFa^G4-2
> UAS-KiR
0.3 ΔF/F0
e
Empty^G4 (n=20)
SIFa^G4 (n=9)
SIFa^G4-2 (n=11)
f
> UAS-SIFaR-RNAi
Empty^G4
SIFaR^G4
PanN^G4
Trpγ^G4
SIFa^G4
g
Empty^G4 (n=12)
SIFaR^G4 (n=15)
PanN^G4 (n=10)
h
> UAS-KiR
Empty^G4 (n=4)
SIFaR^G4 (n=6)
Trpγ^G4 (n=7)
SIFa^G4 (n=9)

Figure 3

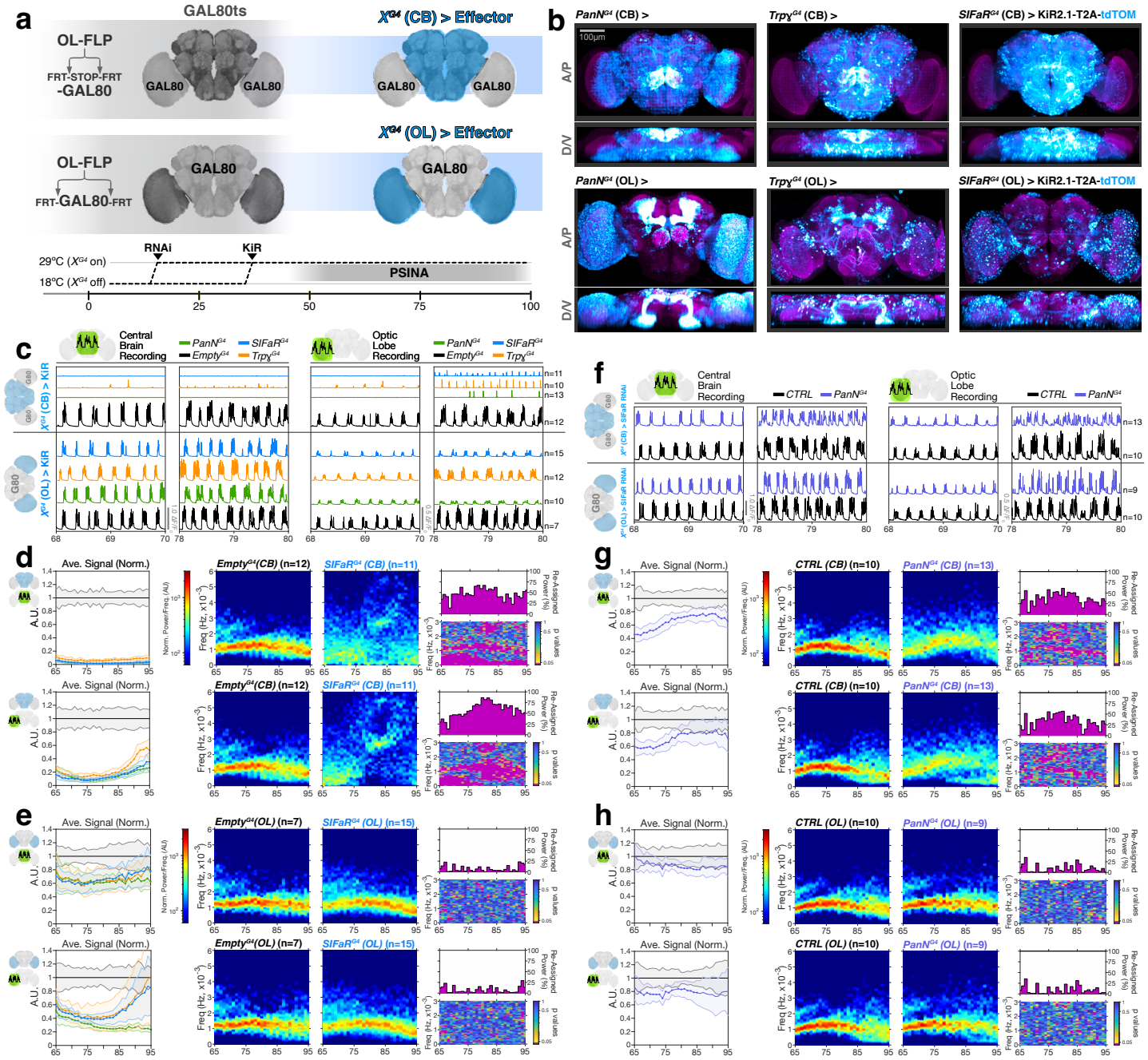
a
GAL80ts
OL-FLP
FRT-STOP-FRT
-GAL80
GAL80
X^G4 (CB) > Effector
X^G4 (OL) > Effector
FRT-GAL80-FRT
RNAi
KiR
29°C (X^G4 on)
18°C (X^G4 off)
PSINA
0
25
50
75
100
b
PanN^G4 (CB) >
Trpγ^G4 (CB) >
SIFaR^G4 (CB) > KiR2.1-T2A-tdTOM
100µm
A/P
D/V
PanN^G4 (OL) >
Trpγ^G4 (OL) >
SIFaR^G4 (OL) > KiR2.1-T2A-tdTOM
c
Central Brain Recording
Optic Lobe Recording
PanN^G4
SIFaR^G4
Empty^G4
Trpγ^G4
X^G4 (CB) > KiR
X^G4 (OL) > KiR
G80
n=11
n=10
n=13
n=12
n=7
d
Ave. Signal (Norm.)
Empty^G4 (CB) (n=12)
SIFaR^G4 (CB) (n=11)
e
Empty^G4 (OL) (n=7)
SIFaR^G4 (OL) (n=15)
f
CTRL
X^G4 (CB) > SIFaR RNAi
X^G4 (OL) > SIFaR RNAi
n=9
g
CTRL (CB) (n=10)
PanN^G4 (CB) (n=13)
h
CTRL (OL) (n=10)
PanN^G4 (OL) (n=9)
A.U.
Freq (Hz, x10^-3)
Re-Assigned Power (%)
p values

Figure 4

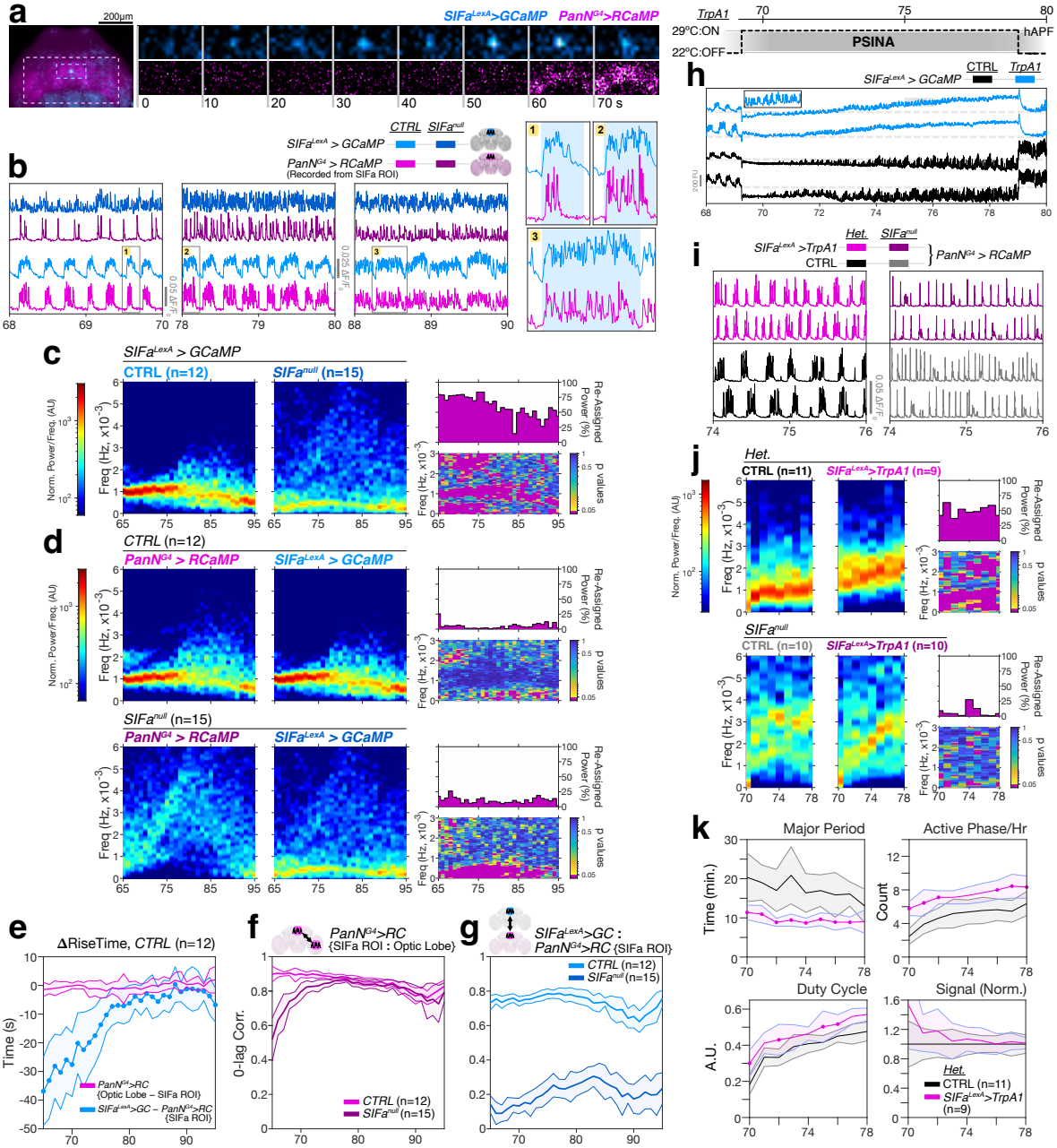
a
200µm
SIFa^LexA>GCaMP PanN^G4>RCaMP
0 10 20 30 40 50 60 70 s
b
CTRL SIFa^null
SIFa^LexA > GCaMP
PanN^G4 > RCaMP
(Recorded from SIFa ROI)
0.05 ΔF/F
0.025 ΔF/F
c
SIFa^LexA > GCaMP
CTRL (n=12)
SIFa^null (n=15)
Norm. Power/Freq. (AU)
Freq (Hz, x10^-3)
Re-Assigned Power (%)
p values
d
CTRL (n=12)
PanN^G4 > RCaMP
SIFa^LexA > GCaMP
SIFa^null (n=15)
e
ΔRiseTime, CTRL (n=12)
Time (s)
PanN^G4>RC (Optic Lobe – SIFa ROI)
SIFa^LexA>GC – PanN^G4>RC (SIFa ROI)
f
PanN^G4>RC (SIFa ROI : Optic Lobe)
0-lag Corr.
CTRL (n=12)
SIFa^null (n=15)
g
SIFa^LexA>GC : PanN^G4>RC (SIFa ROI)
CTRL (n=12)
SIFa^null (n=15)
TrpA1
29ºC:ON
22ºC:OFF
PSINA
hAPF
h
SIFa^LexA > GCaMP
CTRL TrpA1
i
Het. SIFa^null
SIFa^LexA >TrpA1
CTRL
PanN^G4 > RCaMP
0.05 ΔF/F
j
Het.
CTRL (n=11)
SIFa^LexA>TrpA1 (n=9)
SIFa^null
CTRL (n=10)
SIFa^LexA>TrpA1 (n=10)
k
Major Period
Time (min.)
Active Phase/Hr
Count
Duty Cycle
A.U.
Signal (Norm.)
Het.
CTRL (n=11)
SIFa^LexA>TrpA1 (n=9)

Figure 5

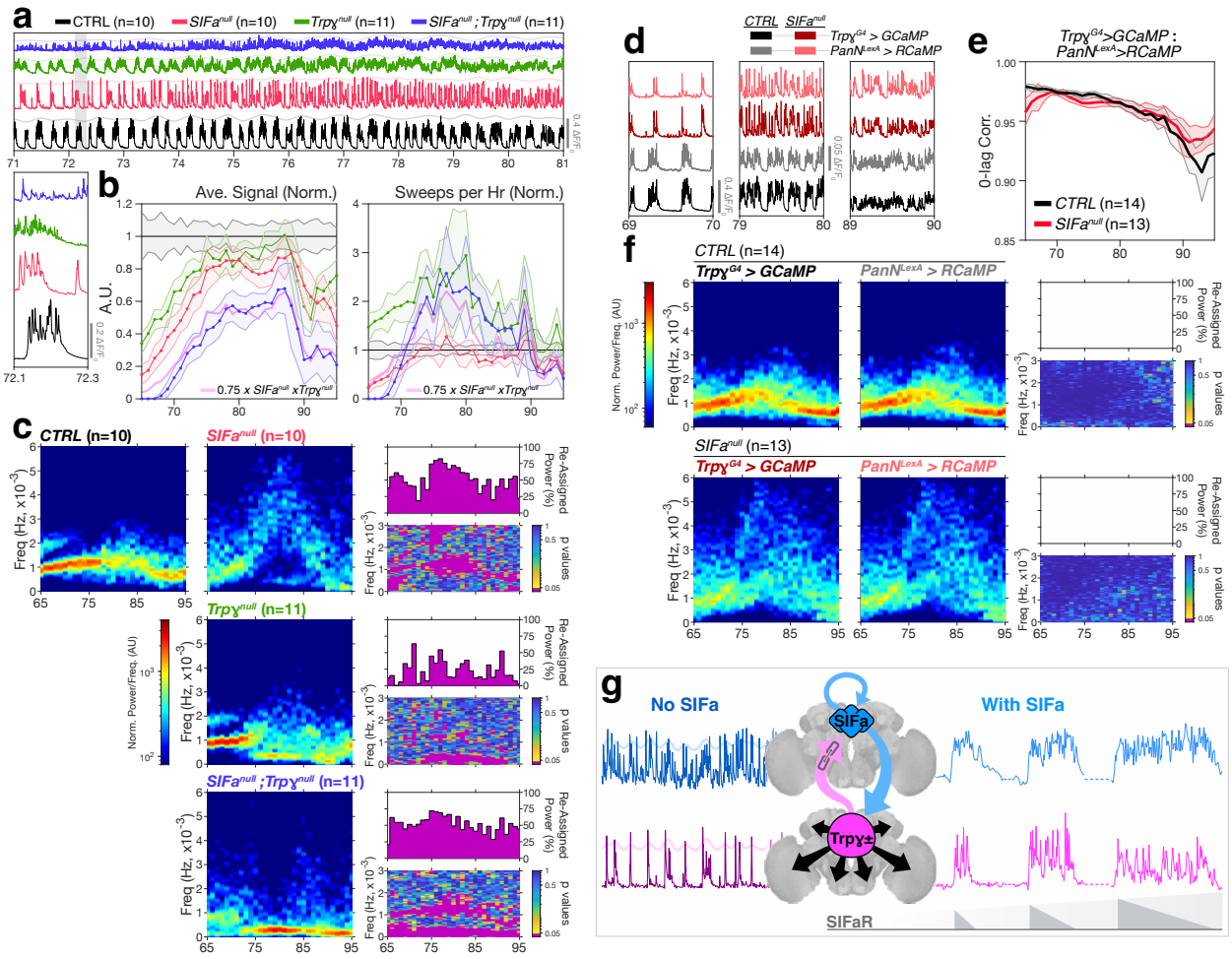
a
CTRL (n=10)
SIFa^null (n=10)
Trpγ^null (n=11)
SIFa^null ;Trpγ^null (n=11)
b
Ave. Signal (Norm.)
Sweeps per Hr (Norm.)
A.U.
0.75 x SIFa^null xTrpγ^null
c
CTRL (n=10)
SIFa^null (n=10)
Trpγ^null (n=11)
SIFa^null ;Trpγ^null (n=11)
Freq (Hz, x10^-3)
Norm. Power/Freq. (AU)
Re-Assigned Power (%)
p values
d
CTRL
SIFa^null
Trpγ^G4 > GCaMP
PanN^LexA > RCaMP
e
Trpγ^G4>GCaMP :
PanN^LexA>RCaMP
0-lag Corr.
CTRL (n=14)
SIFa^null (n=13)
f
CTRL (n=14)
Trpγ^G4 > GCaMP
PanN^LexA > RCaMP
SIFa^null (n=13)
g
No SIFa
With SIFa
SIFa
Trpγ±
SIFaR